

## Original Research Article



# Up-regulation of long non-coding RNA H19 ameliorates renal tubulointerstitial fibrosis by reducing lipid deposition and inflammatory response through regulation of the microRNA-130a-3p/long-chain acyl-CoA synthetase 1 axis

Yali Jiang<sup>1</sup>, Feng Ma<sup>1</sup>, Jing Wang<sup>1</sup>, Xiaojing Chen<sup>1</sup>, Lu Xue<sup>1</sup>, Xinping Chen<sup>1</sup>, Jinping Hu<sup>\*</sup>

Department of Nephrology, Honghui Hospital, Xi'an Jiaotong University, Xi'an, 710054, Shaanxi Province, China

## ARTICLE INFO

## Keywords:

Long-chain acyl-CoA synthetase 1  
lncRNA H19  
Lipid metabolism  
microRNA-130a-3p  
Renal tubulointerstitial fibrosis

## ABSTRACT

Long non-coding RNA (lncRNA) H19 is an extensively studied lncRNA that is related to numerous pathological changes. Our previous findings have documented that serum lncRNA H19 levels are decreased in patients with chronic kidney disorder and lncRNA H19 reduction is closely correlated with renal tubulointerstitial fibrosis, an essential step in developing end-stage kidney disease. Nonetheless, the precise function and mechanism of lncRNA H19 in renal tubulointerstitial fibrosis are not fully comprehended. The present work utilized a mouse model of unilateral ureteral obstruction (UUO) and transforming growth factor- $\beta$ 1 (TGF- $\beta$ 1)-stimulated HK-2 cells to investigate the possible role and mechanism of lncRNA H19 in renal tubulointerstitial fibrosis were investigated. Levels of lncRNA H19 decreased in kidneys of mice with UUO and HK-2 cells stimulated with TGF- $\beta$ 1. Up-regulation of lncRNA H19 in mouse kidneys remarkably relieved kidney injury, fibrosis and inflammation triggered by UUO. Moreover, the increase of lncRNA H19 in HK-2 cells reduced epithelial-to-mesenchymal transition (EMT) induced by TGF- $\beta$ 1. Notably, up-regulation of lncRNA H19 reduced lipid accumulation and triacylglycerol content in kidneys of mice with UUO and TGF- $\beta$ 1-stimulated HK-2 cells, accompanied by the up-regulation of long-chain acyl-CoA synthetase 1 (ACSL1). lncRNA H19 was identified as a sponge of microRNA-130a-3p, through which lncRNA H19 modulates the expression of ACSL1. The overexpression of microRNA-130a-3p reversed the lncRNA H19-induced increases in the expression of ACSL1. The suppressive effects of lncRNA H19 overexpression on the EMT, inflammation and lipid accumulation in HK-2 cells were diminished by ACSL1 silencing or microRNA-130a-3p overexpression. Overall, the findings showed that lncRNA H19 ameliorated renal tubulointerstitial fibrosis by reducing lipid deposition via modulation of the microRNA-130a-3p/ACSL1 axis.

## 1. Introduction

Renal tubulointerstitial fibrosis is an essential step for developing end-stage kidney diseases that still stands as one of the primary reasons for death on a global scale [1]. The incidence of end-stage kidney disorders has continually increased in current years and end-stage kidney disorders affect a lot of the population worldwide, bringing a heavy burden on the family and society [2]. To date, there is still lack of effective therapeutic measures for end-stage kidney diseases. Early intervention in tubulointerstitial fibrosis can delay the progress of chronic kidney disorders to end-stage kidney disorders. Renal tubular

epithelial cells undergo an epithelial-to-mesenchymal transition (EMT) when stimulated by fibrotic cytokines, inflammatory cytokines or chemokines is a key step in developing tubulointerstitial fibrosis [3]. However, there are still limitations in understanding the molecular mechanisms underlying the EMT of renal tubular epithelial cells. Therefore, identifying key regulators and mechanisms for the EMT of renal tubular epithelial cells may contribute to developing innovative and efficacious therapies for preventing tubulointerstitial fibrosis before it becomes irreversible.

Long non-coding RNA (lncRNA) is a category of non-coding RNAs consisting of more than 200 nucleotides, and plays diverse roles in

\* Corresponding author.

E-mail address: [dr\\_hujinping@yeah.net](mailto:dr_hujinping@yeah.net) (J. Hu).

<sup>1</sup> These authors (Yali Jiang, Feng Ma, Jing Wang, Xiaojing Chen, Lu Xue and Xinping Chen) equally to this work.

disease progression [4,5]. lncRNA participates in plenty of cellular processes via its action on gene expression [6]. A well-characterised mechanism of lncRNA in gene expression is the action to sponge microRNAs [7]. microRNAs comprising 19 to 25 nucleotides adjust gene expression after transcription by attaching to the 3'-untranslated region of mRNA, which induces mRNA degradation and inhibits protein synthesis [8]. Therefore, microRNAs serve as an inhibitor of gene expression. By sponging microRNAs, lncRNAs can release the suppressive effect of microRNAs on target genes, thereby enhancing gene expression. lncRNAs have been reported as an emerging contributor to renal tubulointerstitial fibrosis [9,10]. lncRNA H19 is an extensively studied lncRNA that is related to numerous diseases [11–13]. Notably, lncRNA H19 has notable relevance with several kinds of renal disorders [14,15]. However, the function of lncRNA H19 in nephropathy remains elusive.

Lipid metabolism has an essential role in maintaining normal physiological functions and its dysregulation is related to the pathogenesis of numerous disorders [16,17]. The inappropriate buildup of free fatty acids triggers abnormality in lipid metabolism. The entrance of fatty acids into metabolic pathways needs their activation by long chain acyl-CoA synthetases [18]. Fatty acids undergo  $\beta$ -oxidation for energy supply or are utilized for lipid-related biosynthesis only when they are transformed into acyl-CoA by long chain acyl-CoA synthetase [19]. Long-chain acyl-CoA synthetase 1 (ACSL1) is a key member of the long chain acyl-CoA synthetase in lipid catabolism located in the mitochondria and lipid droplets of various tissues [20]. A deficiency of ACSL1 induces lipid deposition in the kidneys, causing lipotoxic injury to renal tubules [21]. Ectopic lipid accumulation in kidneys is closely related to the onset of renal disorders [22]. Excess lipids causes damage to the kidneys, associated with the promotion of an inflammatory response [23]. Moreover, abnormal lipid accumulation is considered to be a major cause of renal tubulointerstitial fibrosis [24–26]. The recovery of normal lipid metabolism has become a promising path for preventing renal tubulointerstitial fibrosis.

lncRNA H19 serves as a key determinant in fibrosis-related disorders [27]. Our previous findings have documented that serum lncRNA H19 levels are decreased in patients with chronic kidney disorders and lncRNA H19 reduction is closely correlated with renal tubulointerstitial fibrosis [28]. Nonetheless, the precise function and mechanism of lncRNA H19 in renal tubulointerstitial fibrosis are not fully comprehended. The present work utilized a mouse model of unilateral ureteral obstruction (UUO) and transforming growth factor- $\beta$ 1 (TGF- $\beta$ 1)-stimulated human proximal tubular epithelial cells HK-2 to investigate the possible role and mechanism of lncRNA H19 in renal tubulointerstitial fibrosis. Levels of lncRNA H19 decreased in kidneys of mice with UUO and TGF- $\beta$ 1-stimulated HK-2 cells. Overexpression of lncRNA H19 in mouse kidneys remarkably relieved the kidney injury, fibrosis and inflammation triggered by UUO. Moreover, the overexpression of lncRNA H19 in HK-2 cells reduced the epithelial-to-mesenchymal transition (EMT) caused by TGF- $\beta$ 1. Notably, the up-regulation of lncRNA H19 reduced lipid accumulation and triacylglycerol content in kidneys of mice with UUO and TGF- $\beta$ 1-stimulated HK-2 cells, accompanied by the up-regulation of ACSL1. Bioinformatic analysis and the luciferase reporter assay identified lncRNA H19 as a sponge of microRNA-130a-3p, through which lncRNA H19 modulated the expression of ACSL1. The suppressive effects of lncRNA H19 overexpression on the EMT, inflammation and lipid accumulation in HK-2 cells induced by TGF- $\beta$ 1 were diminished by ACSL1 silencing or microRNA-130a-3p overexpression. The work showed that lncRNA H19 ameliorated renal tubulointerstitial fibrosis by reducing lipid deposition via modulation of the microRNA-130a-3p/ACSL1 axis.

## 2. Materials and methods

### 2.1. Animal model

Male C57BL/6J mice, aged 6–8 weeks, weighing 18–22 g, were

provided by the Laboratory Animal Center of Xi'an Jiaotong University (Xi'an, China). The mice were raised under a 10/14-h light-dark cycle with rodent chow and drinking water. After acclimatising to this environment for 1 week, mice were subjected to the UUO model construction in accordance with published protocols [29]. Briefly, mice were anaesthetised with inhaled 1.5–2% isoflurane and an incision was made in the upper left quadrant to uncover the left kidney. After isolating the left ureter, it was doubly ligated using 5-0 surgical silk. Sham mice underwent the same surgery without ligation. Meanwhile, 100  $\mu$ l of  $5.0 \times 10^8$  pfu of recombinant adenovirus expressing lncRNA H19 (GenePharma, Shanghai, China) was injected into the kidneys through the left renal artery using a 31-gauge needle. Fourteen days after the surgery, mice were euthanised through intraperitoneal injection of pentobarbital sodium at 150 mg/kg [30]. The kidneys were perfused with PBS and then removed. The isolated kidneys were fixed in 4% paraformaldehyde for an overnight period. Following fixation, the tissues were embedded in paraffin blocks and sliced into 4- $\mu$ m sections for examination of renal histopathology. For frozen section, the kidneys were embedded in optimal cutting temperature compound and snapped-frozen in liquid nitrogen using a cryostat. Tissues were then sliced into 10- $\mu$ m sections using a constant temperature freezing microtome for determination of lipid accumulation. The animal protocols were reviewed and approved by the Institutional Animal Care and Use Committee of Honghui Hospital and complied with the guidelines of the National Research Council's Guide for the Care and Use of Laboratory Animals.

### 2.2. Cell culture and treatment

HK-2 and 293T cells were provided by Procell (Wuhan, China) and maintained according to the manufacturer's guidelines. To construct an *in vitro* fibrosis model, HK-2 cells were stimulated with TGF- $\beta$ 1 at 50 ng/ml for 48 h. Recombinant adenoviruses were transduced into HK-2 cells at a multiplicity of infection of 100. ACSL1 siRNAs, microRNA-130a-3p mimics or the corresponding controls were transfected into cells using TransIntro Transfection Reagent (TransGen, Beijing, China) following the protocols provided by the manufacturer.

### 2.3. Quantitative real-time polymerase chain reaction

Total RNAs in kidney samples or cells were isolated with TRIzol. microRNAs were purified and enriched by EasyPure miRNA Kit (TransGen Biotech, Beijing, China). Reverse transcription for total RNAs was performed with TransScript First-Strand cDNA Synthesis SuperMix, while reverse transcription for microRNAs was performed with TransScript miRNA First-Strand cDNA Synthesis SuperMix (TransGen Biotech). Quantitative real-time polymerase chain reaction was performed using PerfectStart Green qPCR SuperMix (TransGen Biotech). Each sample was quantified in triplicate and normalised to glyceraldehyde-3-phosphate dehydrogenase (GAPDH) (for mRNA and lncRNA) or U6 (for microRNA). Expression levels were expressed as fold changes relative to control group using the formula  $2^{-\Delta\Delta Ct}$ .

### 2.4. Renal function and histopathology

The concentration of creatinine and blood urea nitrogen in mice serum was quantified by Creatinine and Urea Assay Kits (Jiancheng Bioengineering Institute, Nanjing, China). Fixed-kidney samples were embedded into paraffin and sliced into 4- $\mu$ m slices. The slices were mounted onto glass slides followed by deparaffinisation and rehydration with standard protocols. Thereafter, the slices were stained with haematoxylin dye solution and 1% eosin alcohol. After washing with distilled water, the slices were dehydrated and cleaned. The slides were sealed with mounting medium and the histopathology was detected by a microscope. To determine renal fibrosis, renal slices were subjected to Masson's trichrome staining using Masson's Trichrome Stain Kit (Solarbio, Beijing, China) To measure collagen deposition, renal slices

were subjected to Sirius red staining using Modified Sirius Red Stain Kit (Solarbio) according to the manufacturer's instructions. The intensity of fibrosis and collagen deposition was measured using Image-Pro Plus 6.0 software. The results were normalised to the control group to obtain the relative intensity.

### 2.5. Oil Red O staining

The determination of lipid accumulation was performed using the Oil Red O staining with Modified Oil Red O Stain Kit (Solarbio). For cultured cells, cells were fixed by 4 % paraformaldehyde. Tissue freezing medium-embedded frozen kidney samples were sliced into 10- $\mu$ m sections. Cells or slices were stained with Oil Red O solution for 20 min. Following rinsing with phosphate buffered saline, the samples were examined using a microscope.

### 2.6. Determination of triglyceride content

Triglyceride content was determined using Triglyceride Content Assay Kit (Solarbio). Kidney samples (10 mg) or cultured cells ( $6 \times 10^6$ ) were homogenised in 1 ml of lysis buffer. The supernatants were collected by centrifugation and triglyceride contents were measured by colorimetry according to the kit instructions.

### 2.7. Western blotting

Proteins isolated from kidney samples or cultured cells were separated on 12 % sodium dodecyl sulfate-polyacrylamide gel, transferred to nitrocellulose membranes and blocked with 5 % skim milk. Immunoblotting was performed using the primary antibodies and horseradish peroxidase-conjugated secondary antibodies. Blots were visualised by enhanced chemiluminescence kit (Zhonghui Hecai Biotech, Xi'an, China) and images were captured by a Bio-Rad Imaging System. Antibodies used were as follows: anti-P65 (CST, Shanghai, China), anti-p-P65 (CST), anti-ACSL1 (Sanying Biotech, Wuhan, China), anti-E-cadherin (Sanying Biotech), anti- $\alpha$ -smooth muscle actin (Sanying Biotech), anti-fibronectin (Sanying Biotech), anti-GAPDH (Sanying Biotech) and horseradish peroxidase-conjugated goat anti-rabbit IgG (Sanying Biotech). Band intensities were quantified using densitometry analysis with Image-Pro Plus 6.0 software. The value of target protein intensity/glyceraldehyde-3-phosphate dehydrogenase intensity was normalised to that of control group to obtain the relative expression of target proteins.

### 2.8. Enzyme-linked immunosorbent assay

The levels of tumor necrosis factor- $\alpha$ , interleukin-6 and interleukin-1 $\beta$  in kidney samples or cultured cells were assessed with specific enzyme-linked immunosorbent assay kits (Elabscience, Wuhan, China) in according to the kit instructions.

### 2.9. Bioinformatic analysis and luciferase reporter assay

The microRNAs that targets ACSL1 were predicted using TargetScan ([https://www.targetscan.org/vert\\_80/](https://www.targetscan.org/vert_80/)) [31]. The binding sites in ACSL1 3'-untranslated region for microRNA-130a-5p are 5'-UUG-CACU-3'. The microRNAs that targets lncRNA H19 were predicted using Encyclopedia of RNA Interactomes (<https://starbase.sysu.edu.cn/>) [32]. The binding sites in lncRNA H19 for microRNA-130a-5p are 5'-UUG-CACU-3'. lncRNA H19 or 3'-untranslated region of ACSL1 cDNA fragments which contain the predicted binding sites of microRNA-130a-3p sites, were subcloned into dual-luciferase reporter plasmids. The dual-luciferase reporter plasmids and microRNA-130a-3p mimics or negative control mimics were co-transfected into 293T cells using TransIntro Transfection Reagent (TransGen). After a 48-h incubation period, the luciferase activity was measured by means of the Dual

Luciferase Reporter Gene Assay Kit II (Beyotime, Shanghai, China).

### 2.10. RNA pull-down assay

Biotinylated negative control mimics or microRNA-130a-3p mimics were prepared using Biotin RNA Labelling Mix (Roche Diagnostics). Biotin-labelled mimics were then introduced in HK-2 cells, followed by incubation for 48 h. After lysing the cells, they were incubated with Streptavidin-Coated Magnetic Beads at 4 °C overnight. The RNA bound to the beads was extracted and purified for quantitative real-time polymerase chain reaction.

### 2.11. Statistical analysis

Experimental data depicted in graphs represented mean  $\pm$  standard deviation. The experiments were conducted a minimum of three times. Data analysis was conducted using the Student's t-test or one-way analysis of variance with Tukey's post-hoc test. GraphPad Prism 8 was used for statistical analysis. The threshold for significance was set at  $p < 0.05$ .

## 3. Results

### 3.1. Up-regulation of lncRNA H19 alleviates the development of renal tubulointerstitial fibrosis

The work primarily examines whether lncRNA H19 levels change in kidneys with UO compared to normal kidneys. The results showed that lncRNA H19 levels were markedly decreased in kidneys from UO mice versus sham mice (Fig. 1A). lncRNA H19 reduction in the UO model indicates a potential connection between lncRNA H19 and renal tubulointerstitial fibrosis. To investigate the exact role of lncRNA H19 in renal tubulointerstitial fibrosis, H19 was overexpressed in mice with UO by adenoviral-mediated gene transfer. Levels of lncRNA H19 were significantly up-regulated in mice infected with recombinant adenoviruses expressing lncRNA H19 (Fig. 1B). Serum creatinine and blood urea nitrogen were increased in mice with UO, which were markedly decreased by lncRNA H19 overexpression (Fig. 1C and D). Haematoxylin-eosin staining revealed severe tubulointerstitial damages with tubular dilatation and swelling and increased inflammatory cell infiltration in UO kidneys, while these pathological features were remarkably reversed by lncRNA H19 overexpression in UO mice (Fig. 1E). Sirius Red staining revealed massive collagen fibre formation in UO kidneys, which was markedly reversed by lncRNA H19 overexpression (Fig. 1E and F). Masson staining further showed increased fibrosis area in UO kidneys, which was significantly reversed by lncRNA H19 overexpression (Fig. 1E and G). Overall, these findings suggest that lncRNA H19 possesses the capability to safeguard against renal tubulointerstitial fibrosis.

### 3.2. Up-regulation of lncRNA H19 restrained the EMT of tubular epithelial cells

The EMT of renal tubular epithelial cells is a key step in the development of tubulointerstitial fibrosis. Under sham condition, overexpression of lncRNA H19 showed no significant effect on the baseline of the epithelial cell marker E-cadherin, the mesenchymal cell marker  $\alpha$ -smooth muscle actin and fibrosis marker fibronectin (Fig. 2A–D). Notably, E-cadherin was decreased, while  $\alpha$ -smooth muscle actin and fibronectin were increased in UO kidneys (Fig. 2A–D). Comparatively, E-cadherin was increased, while  $\alpha$ -smooth muscle actin and fibronectin were decreased in UO kidneys by lncRNA H19 overexpression in mice (Fig. 2A–D). To further verify the relationship between lncRNA H19 and renal tubulointerstitial fibrosis, we constructed an *in vitro* model of renal tubulointerstitial fibrosis by stimulating HK-2 cells with TGF- $\beta$ 1. We first examined the alterations in lncRNA H19 expression in response to TGF-

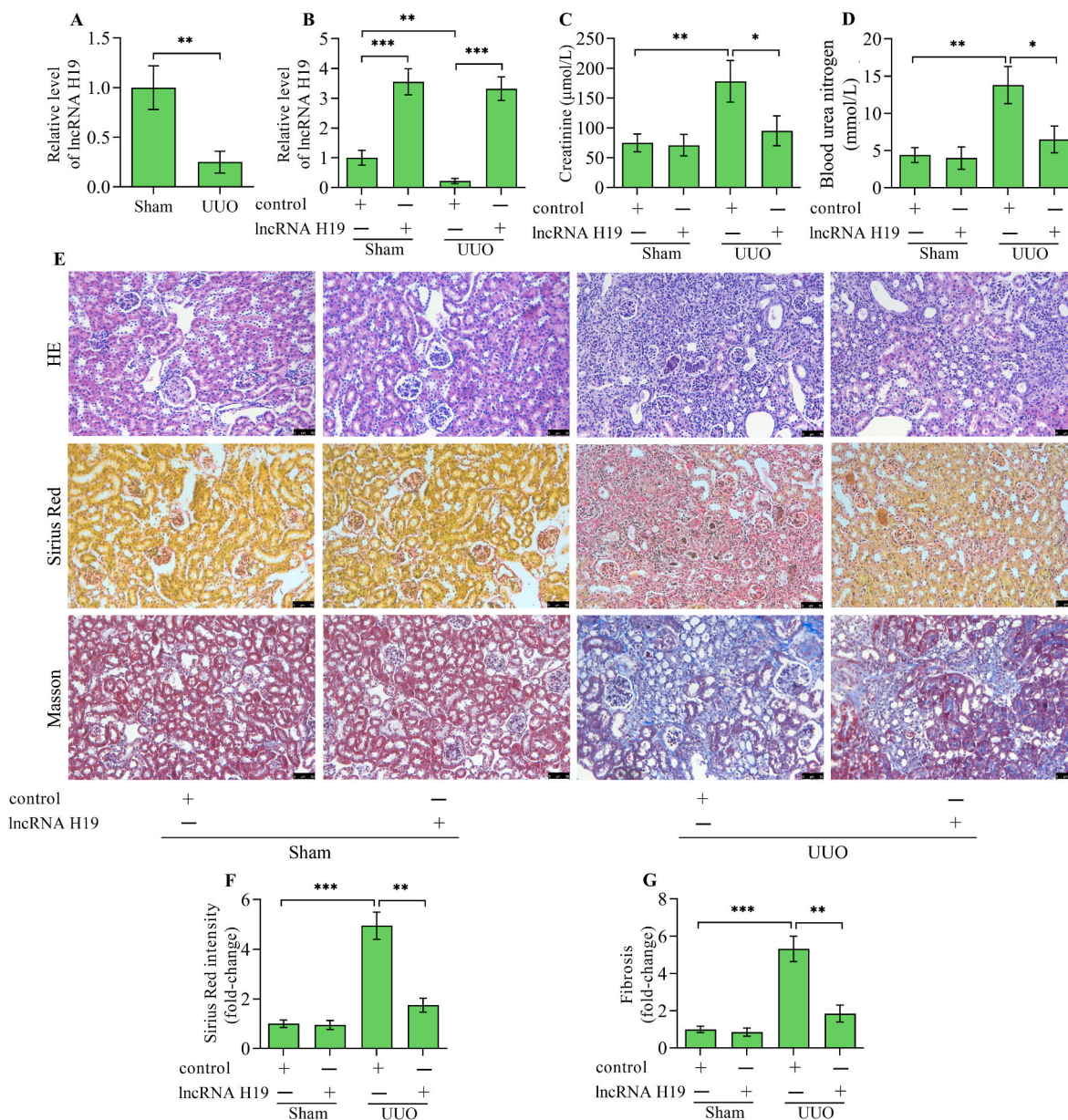


**Fig. 1.** Effect of lncRNA H19 overexpression on renal tubulointerstitial fibrosis. (A) Quantitative real-time polymerase chain reaction detection of lncRNA H19 levels in kidneys from UUO and sham mice (n = 3). (B) Quantitative real-time polymerase chain reaction detection of lncRNA H19 levels in kidneys from sham and UUO mice infected with adenoviruses expressing lncRNA H19 or control adenoviruses (n = 3). The levels of (C) creatinine and (D) blood urea nitrogen in sham and UUO mice infected with adenoviruses expressing lncRNA H19 or control adenoviruses (n = 3). (E) Haematoxylin-eosin staining, Sirius Red staining and Masson staining of kidney tissues from sham and UUO mice infected with adenoviruses expressing lncRNA H19 or control adenoviruses. (F) The intensity of Sirius Red staining was quantitatively analyzed (n = 3). (G) The fibrosis intensity was quantitatively analyzed (n = 3). Data were presented as mean ± standard deviation, \*p < 0.05, \*\*p < 0.01 and \*\*\*p < 0.001. UUO, unilateral ureteral obstruction; HE, haematoxylin-eosin.

β1 stimulation. Compared with unstimulated cells, H19 levels significantly decreased in response to TGF-β1 stimulation (Fig. 2E). To overexpress lncRNA H19 in HK-2 cells, we conducted transduction using adenoviruses expressing lncRNA H19. Transduction of adenoviruses expressing lncRNA H19 markedly elevated levels of lncRNA H19 in HK-2 cells with or without TGF-β1 stimulation (Fig. 2F). The induction of EMT by TGF-β1 was evidenced by a decrease in E-cadherin expression and an increase in α-smooth muscle actin and fibronectin levels (Fig. 2G–J). Notably, the overexpression of lncRNA H19 markedly restored E-cadherin and reduced α-smooth muscle actin and fibronectin in HK-2 cells stimulated with TGF-β1 (Fig. 2G–J). However, lncRNA H19 overexpression showed no significant effect on the expression of E-cadherin, α-smooth muscle actin and fibronectin in HK-2 cells without

TGF-β1 stimulation. These observations indicate that lncRNA H19 may specifically influence the EMT exclusively when it is initiated, rather than serving as an initiator of this process. Altogether, these findings indicate that lncRNA H19 is involved in regulating the EMT of tubular epithelial cells.

### 3.3. Up-regulation of lncRNA H19 relieves inflammatory response during renal tubulointerstitial fibrosis

High levels of inflammatory cytokine production are correlated with the development of renal tubulointerstitial fibrosis. The levels of tumor necrosis factor-α, interleukin-6 and interleukin-1β, elevated in UUO kidneys were markedly lowered by lncRNA H19 overexpression

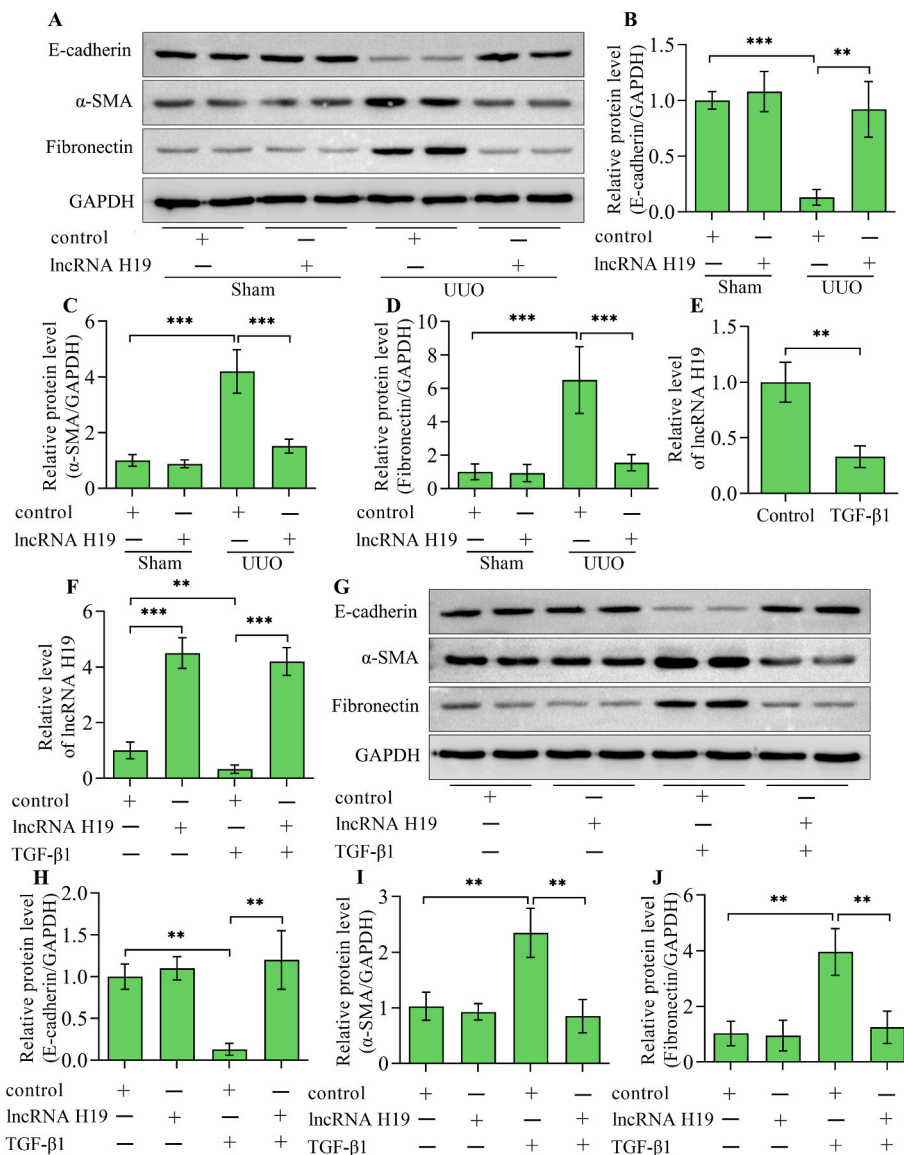


**Fig. 2.** Effect of lncRNA H19 overexpression on the EMT of renal tubular epithelial cells. (A) Western blotting detection and quantification of (B) E-cadherin, (C)  $\alpha$ -smooth muscle actin and (D) fibronectin in kidneys from sham and UUO mice infected with adenoviruses expressing lncRNA H19 or control adenoviruses ( $n = 3$ ). (E) Quantitative real-time polymerase chain reaction detection of lncRNA H19 levels in HK-2 cells with or without TGF- $\beta$ 1 stimulation. HK-2 cells were infected with adenoviruses expressing lncRNA H19 or control adenoviruses and then subjected to TGF- $\beta$ 1 stimulation ( $n = 3$ ). (F) Quantitative real-time polymerase chain reaction detection of lncRNA H19 levels after adenoviruses infection in HK-2 cells stimulated with TGF- $\beta$ 1 ( $n = 3$ ). (G) Western blotting and quantification of (H) E-cadherin, (I)  $\alpha$ -smooth muscle actin and (J) fibronectin ( $n = 3$ ). Data were presented as mean  $\pm$  standard deviation, \*\* $p < 0.01$  and \*\*\* $p < 0.001$ . UUO, unilateral ureteral obstruction;  $\alpha$ -SMA,  $\alpha$ -smooth muscle actin; GAPDH, glyceraldehyde-3-phosphate dehydrogenase; TGF- $\beta$ 1, transforming growth factor- $\beta$ 1.

(Fig. 3A–C). Moreover, the inflammation-related transcription factor nuclear factor- $\kappa$ B P65 activated in UUO kidneys was also reduced by lncRNA H19 overexpression (Fig. 3D and E). In addition, the increases in tumor necrosis factor- $\alpha$ , interleukin-6, interleukin-1 $\beta$  (Fig. 3F–H), and phosphorylated P65 (Fig. 3I and J) in HK-2 cells stimulated with TGF- $\beta$ 1 were also reversed by lncRNA H19 overexpression. Overall, these results suggest that lncRNA H19 regulates the inflammatory response in the progression of renal tubulointerstitial fibrosis.

### 3.4. Up-regulation of lncRNA H19 reduces lipid deposition in renal tubulointerstitial fibrosis

Ectopic lipid deposition exerts a crucial role in the development of renal tubulointerstitial fibrosis. Considering that lncRNA H19 has a role in lipid metabolism, the work assessed whether lncRNA H19 affects lipid deposition in kidneys with tubulointerstitial fibrosis. Oil Red O staining

revealed excess lipid deposition in UUO kidneys, which was remarkably reversed by lncRNA H19 overexpression (Fig. 4A and B). Moreover, triglyceride content increased in UUO kidneys was also reduced by lncRNA H19 overexpression (Fig. 4C). In vitro studies also demonstrated that an excess of lipid deposition (Fig. 4D and E) and triglyceride content (Fig. 4F) in HK-2 cells stimulated with TGF- $\beta$ 1 was markedly down-regulated by lncRNA H19 overexpression. Collectively, these findings indicate that lncRNA H19 regulates lipid deposition during the progression of renal tubulointerstitial fibrosis.

### 3.5. lncRNA H19 mediates suppression of lipid deposition by ACSL1

ACSL1 is a key enzyme for lipid metabolism which reduces the accumulation of lipids by activating long-chain fatty acids. ACSL1 levels were decreased in UUO kidneys, which were restored by lncRNA H19 overexpression (Fig. 5A–C). Overexpression of lncRNA H19 also up-

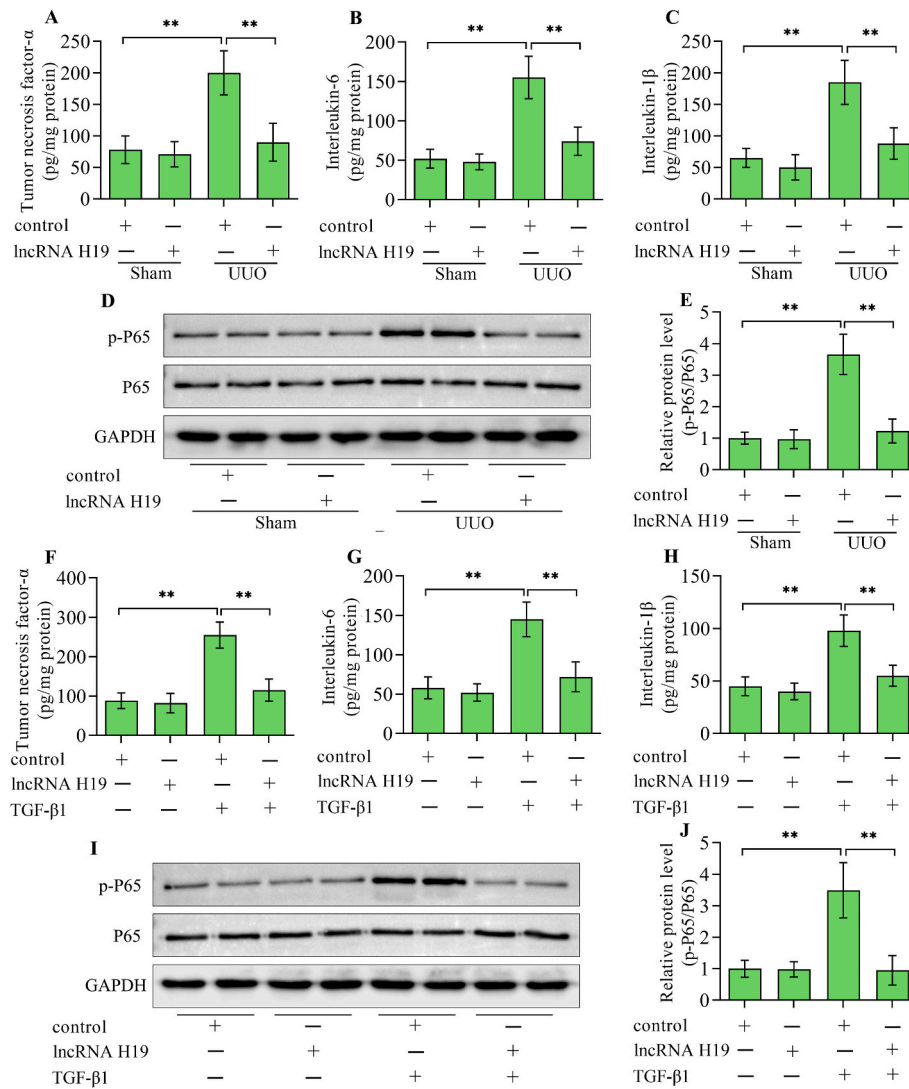


**Fig. 3.** Effect of lncRNA H19 overexpression on inflammatory response. Enzyme-linked immunosorbent assay detection of (A) tumor necrosis factor- $\alpha$ , (B) interleukin-6 and (C) interleukin-1 $\beta$  in kidneys from sham and UUO mice infected with adenoviruses expressing lncRNA H19 or control adenoviruses ( $n = 3$ ). (D) Western blotting detection and (E) quantification of nuclear factor- $\kappa$ B P65 in kidneys from sham and UUO mice infected with adenoviruses expressing lncRNA H19 or control adenoviruses ( $n = 3$ ). Enzyme-linked immunosorbent assay detection of (F) tumor necrosis factor- $\alpha$ , (G) interleukin-6 and (H) interleukin-1 $\beta$  in HK-2 cells infected with adenoviruses expressing lncRNA H19 or control adenoviruses following TGF- $\beta$ 1 stimulation ( $n = 3$ ). (I) Western blotting detection and (J) quantification of nuclear factor- $\kappa$ B P65 in HK-2 cells infected with adenoviruses expressing lncRNA H19 or control adenoviruses following TGF- $\beta$ 1 stimulation ( $n = 3$ ). Data were presented as mean  $\pm$  standard deviation,  $**p < 0.01$ . UUO, unilateral ureteral obstruction; P65, nuclear factor- $\kappa$ B P65; GAPDH, glyceraldehyde-3-phosphate dehydrogenase; TGF- $\beta$ 1, transforming growth factor- $\beta$ 1.

regulated the expression of ACSL1 in HK-2 cells stimulated with TGF- $\beta$ 1 (Fig. 5D–F). Moreover, the silencing of ACSL1 (Fig. 5G and H) diminished the suppressive effect of lncRNA H19 overexpression on lipid accumulation induced by TGF- $\beta$ 1 (Fig. 5I and J). In addition, the suppressive impacts of lncRNA H19 overexpression on the EMT (Fig. 6A–D) and inflammatory response (Fig. 6E and F) induced by TGF- $\beta$ 1 were also reversed by silencing ACSL1. Overall, these results suggest that lncRNA H19 regulates lipid deposition through the regulation of ACSL1.

### 3.6. lncRNA H19 increases the expression of ACSL1 by sponging microRNA-130a-3p

A binding site for microRNA-130a-3p in lncRNA H19 and 3'-untranslated region of ACSL1 was predicted through bioinformatic analysis. (Fig. 7A). A luciferase reporter assay demonstrated that microRNA-130a-3p mimics markedly reduced the luciferase activity of wild-type lncRNA H19 reporter plasmid, while it had no obvious effect on the

mutant lncRNA H19 reporter plasmid (Fig. 7B). Results of RNA pull-down assay demonstrated a significant enrichment of lncRNA H19 in biotinylated microRNA-130a-3p mimic-precipitated RNAs compared with biotinylated negative mimic-precipitated RNA transcripts (Fig. 7C). Moreover, the direct interaction between microRNA-130a-3p and 3'-untranslated region of ACSL1 was verified by the luciferase reporter assay (Fig. 7D). The transfection of microRNA-130a-3p mimics into TGF- $\beta$ 1-stimulated HK-2 cells decreased the level of ACSL1 (Fig. 7E and F). Furthermore, the lncRNA H19-induced up-regulation of ACSL1 level in TGF- $\beta$ 1-stimulated HK-2 cells was markedly reversed by microRNA-130a-3p mimics transfection (Fig. 7E and F). Altogether, these findings indicate that lncRNA H19 regulates the expression of ACSL1 by sponging microRNA-130a-3p.

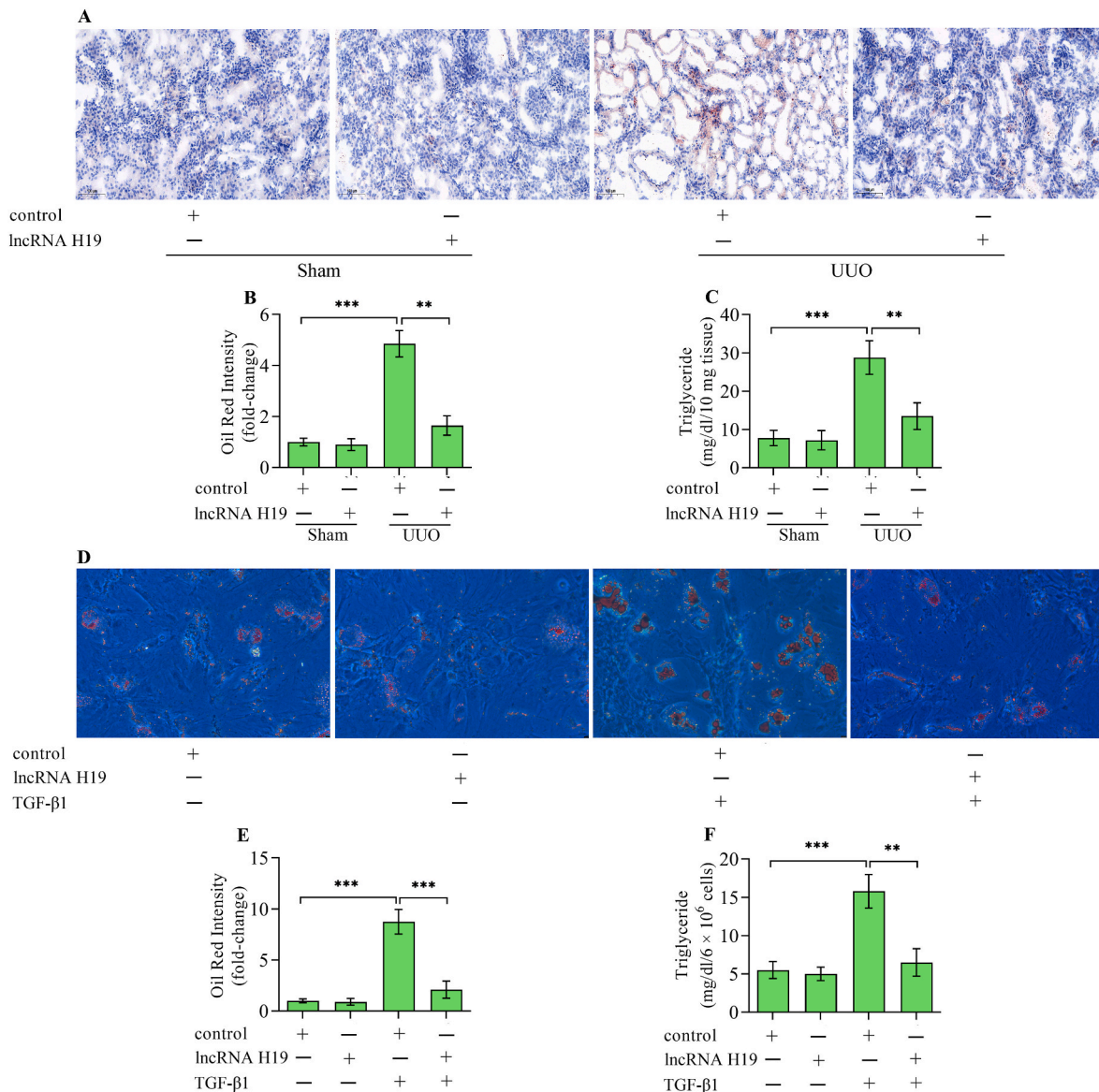


**Fig. 4.** Effect of lncRNA H19 overexpression on lipid deposition. (A, B) Oil Red O staining of lipid deposition in kidneys from sham and UUO mice infected with adenoviruses expressing lncRNA H19 or control adenoviruses (n = 3). (C) Triglyceride content in kidneys from sham and UUO mice infected with adenoviruses expressing lncRNA H19 or control adenoviruses (n = 3). (D, E) Oil Red O staining of lipid deposition in HK-2 cells infected with adenoviruses expressing lncRNA H19 or control adenoviruses following TGF-β1 stimulation (n = 3). (F) Triglyceride content in HK-2 cells infected with adenoviruses expressing lncRNA H19 or control adenoviruses following TGF-β1 stimulation (n = 3). Data were presented as mean ± standard deviation, \*\*p < 0.01 and \*\*\*p < 0.001. UUO, unilateral ureteral obstruction; TGF-β1, transforming growth factor-β1.

### 3.7. Up-regulation of microRNA-130a-3p reverses lncRNA H19-mediated effects on lipid deposition, EMT and inflammatory response

To verify whether microRNA-130a-3p contributes to lncRNA H19-mediated effects on renal fibrosis, the impacts of microRNA-130a-3p overexpression on lncRNA H19-overexpression-mediated lipid deposition, EMT and inflammatory response in TGF-β1-stimulated HK-2 cells were assessed. The transfection of microRNA-130a-3p mimics into HK-2 cells enhanced the lipid deposition (Fig. 8A and B), EMT (Fig. 8C–F) and inflammatory response (Fig. 8G and H) triggered by TGF-β1. Notably, lncRNA H19-induced suppressive effects on TGF-β1-triggered lipid deposition (Fig. 8A and B), EMT (Fig. 8C–F) and inflammatory response (Fig. 8G and H) were markedly diminished by microRNA-130a-3p overexpression. Collectively, these results suggest that microRNA-130a-3p contributes to lncRNA H19-mediated effects on lipid deposition, EMT and inflammatory response triggered by TGF-β1 in HK-2 cells.

## 4. Discussion

The present work delineates a novel mechanism for lncRNA H19 in renal tubulointerstitial fibrosis. The up-regulation of lncRNA H19 alleviated renal tubulointerstitial fibrosis and the EMT of renal tubular epithelial cells, accompanied by a reduction of lipid deposition and inflammatory response. lncRNA H19 was capable of increasing the expression of ACSL1 by sponging microRNA-130a-3p, through which lncRNA H19 restrained lipid deposition, leading to the suppression of EMT of renal tubular epithelial cells and inflammatory response, which could prevent renal tubulointerstitial fibrosis (Fig. 9).

lncRNA H19 has been reported to be a pivotal regulator of fibrosis-related diseases [27,33]. However, the role of lncRNA H19 in fibrosis remains paradoxical. Both pro-fibrotic and anti-fibrotic functions of lncRNA H19 are found in different organs [27]. Therefore, lncRNA H19 may regulate fibrosis in a context-dependent manner, meaning that its

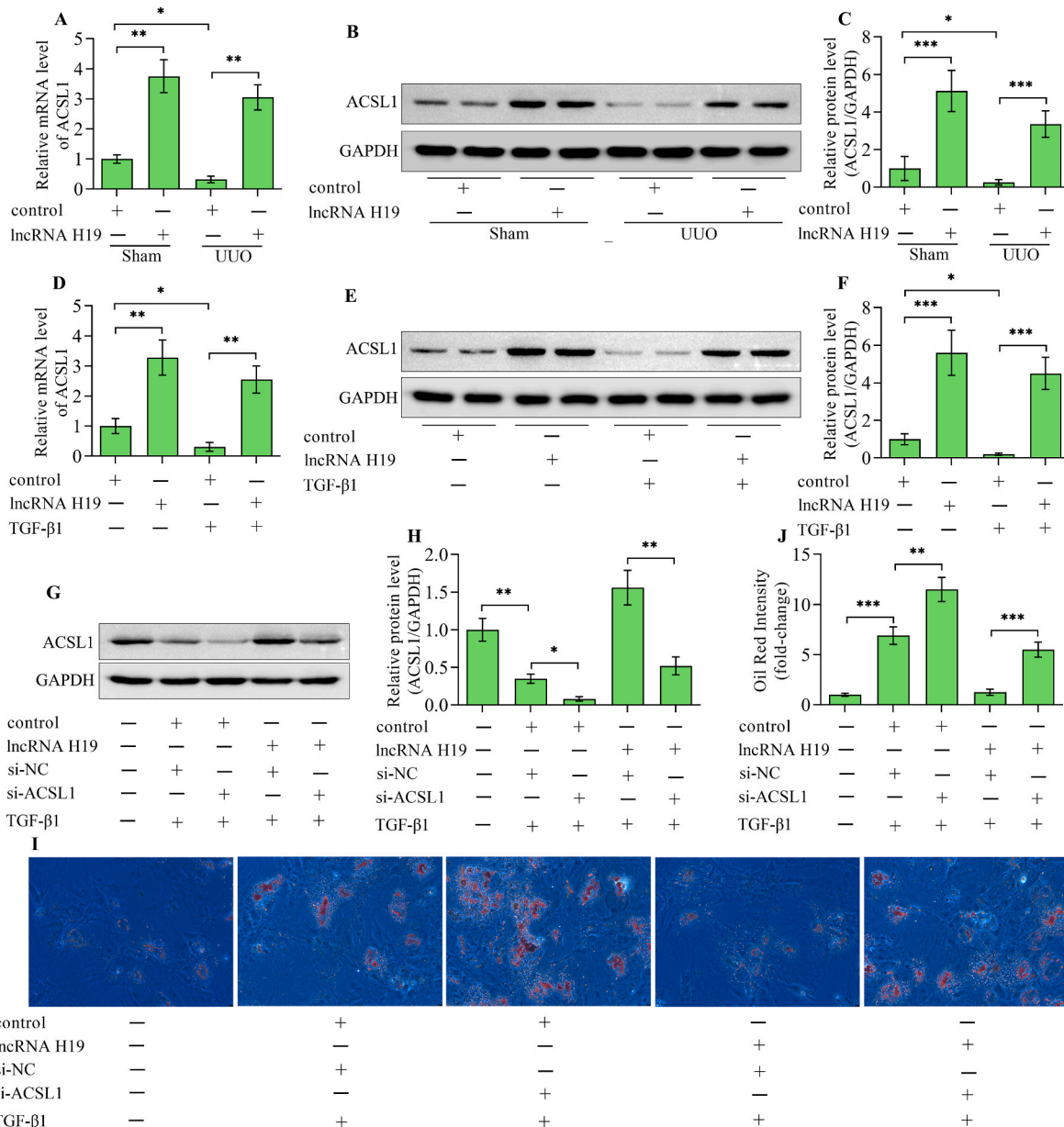


**Fig. 5.** ACSL1 is essential for lncRNA H19-mediated suppression of lipid deposition. (A) Quantitative real-time polymerase chain reaction and (B, C) Western blotting detection of ACSL1 in kidneys from sham and UUO mice infected with adenoviruses expressing lncRNA H19 or control adenoviruses (n = 3). (D) Quantitative real-time polymerase chain reaction and (E, F) Western blotting detection of ACSL1 in HK-2 cells infected with adenoviruses expressing lncRNA H19 or control adenoviruses following TGF-β1 stimulation (n = 3). (G, H) Cells were co-transfected with ACSL1 siRNA or negative control siRNA and adenoviruses expressing lncRNA H19 or control adenoviruses before stimulated with TGF-β1 and the level of ACSL1 was examined by Western blotting (n = 3). (I, J) Oil Red O staining of lipid deposition in cells with various treatments were shown (n = 3). Data were presented as mean ± standard deviation, \*p < 0.05, \*\*p < 0.01 and \*\*\*p < 0.001. UUO, unilateral ureteral obstruction; ACSL1, long-chain acyl-CoA synthetase 1; GAPDH, glyceraldehyde-3-phosphate dehydrogenase; TGF-β1, transforming growth factor-β1; si-NC, negative control siRNA; si-ACSL1, long-chain acyl-CoA synthetase 1 siRNA.

exact effect on fibrosis needs further investigation using different models. Our previous study found that lncRNA H19 levels were decreased in the serum of patients with chronic kidney diseases and lncRNA H19 reduction was closely related to renal tubulointerstitial fibrosis [28]. In this work, we further investigated the exact role of lncRNA H19 in renal tubulointerstitial fibrosis using the UUO mouse model *in vivo*. Decreased levels of lncRNA H19 were shown in kidneys from mice with UUO. The up-regulation of lncRNA H19 in mouse kidneys significantly ameliorated the renal damage and tubulointerstitial fibrosis in mice with UUO. The fibrosis of renal tubular epithelial cells is a key step in developing renal tubulointerstitial fibrosis. The profibrotic response in renal tubular epithelial cells induced by TGF-β1 has been

extensively utilized as an *in vitro* model to study renal tubulointerstitial fibrosis [34–37]. The EMT triggered by TGF-β1 closely mimics a crucial pathological event in the progression of renal tubulointerstitial fibrosis [38]. In this work, we constructed the *in vitro* model of renal tubulointerstitial fibrosis by stimulating human renal proximal tubular epithelial cells HK-2 with TGF-β1. Our results demonstrated that lncRNA H19 levels were decreased in TGF-β1-stimulated HK-2 cells. Consistently, previous findings have demonstrated that TGF-β1 negatively modulates lncRNA H19 expression [39,40]. TGF-β1 stimulation in HK-2 cells triggered EMT, which was markedly reversed by increasing lncRNA H19 expression. Therefore, these results illustrate a renal-protective and anti-fibrotic function of lncRNA H19. However, our findings are



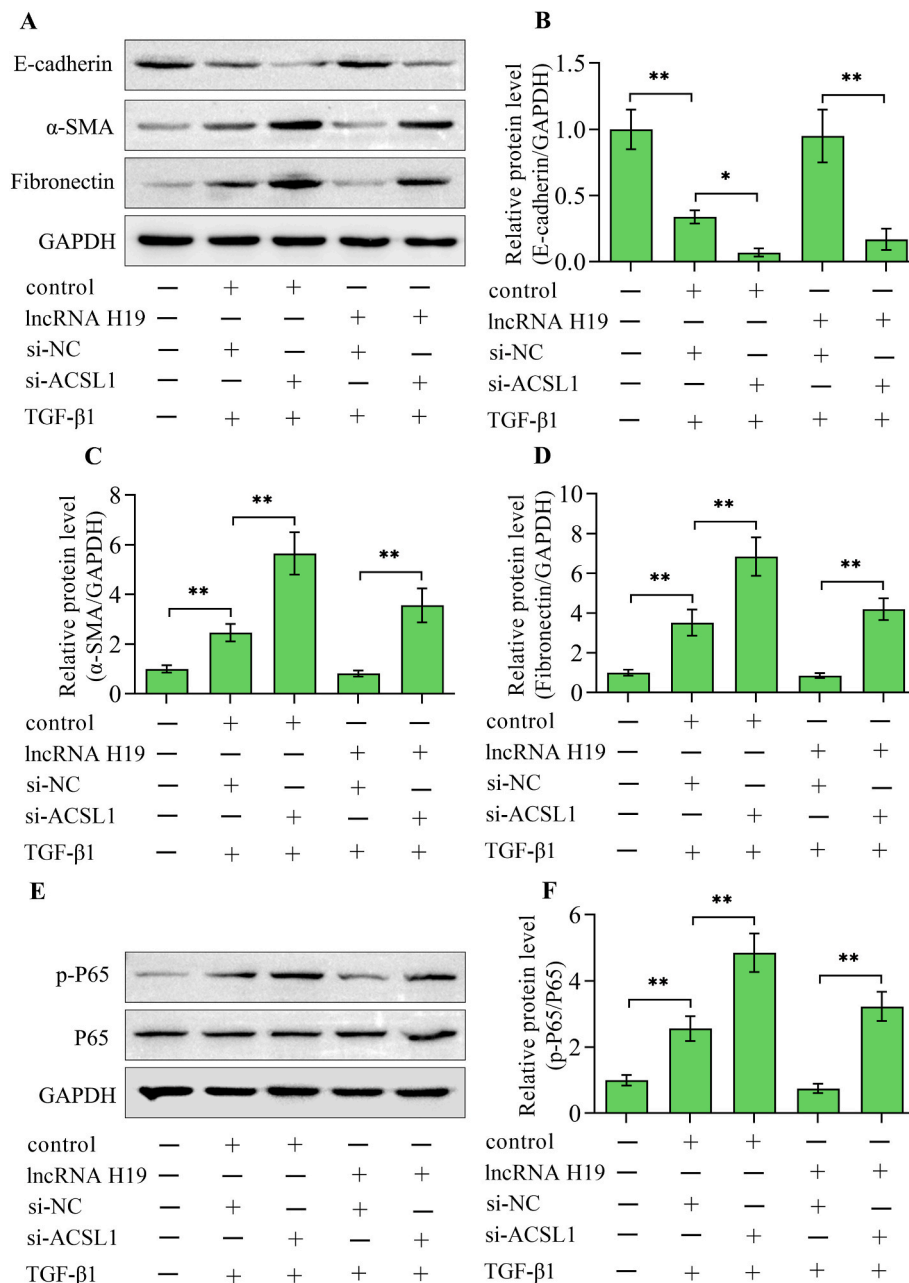


**Fig. 6.** Silencing of ACSL1 abolished the lncRNA H19-mediated suppression of TGF-β1-induced EMT and inflammatory response. (A) Western blotting detection and quantification of (B) E-cadherin, (C) α-smooth muscle actin and (D) fibronectin in HK-2 cells with different treatments (n = 3). (E, F) Western blotting detection and quantification of nuclear factor-κB P65 in cells with various treatments (n = 3). Data were presented as mean ± standard deviation, \*p < 0.05 and \*\*p < 0.01. α-SMA, α-smooth muscle actin; GAPDH, glyceraldehyde-3-phosphate dehydrogenase; TGF-β1, transforming growth factor-β1; si-NC, negative control siRNA; si-ACSL1, long-chain acyl-CoA synthetase 1 siRNA; P65, nuclear factor-κB P65.

different from recent studies which report an enhancing role of lncRNA H19 on renal fibrosis [14,41]. lncRNA H19 was shown to facilitate the transition from ischemia-induced acute kidney injury to chronic kidney disorder by promoting kidney fibrosis [14]. Under diabetic conditions, the high expression of lncRNA H19 contributed to the development of fibrotic kidneys [41]. Therefore, lncRNA H19 may intervene in the development of kidney fibrosis in a context-dependent manner.

ACSL1 serves as a key player in lipid metabolism by accelerating fatty acid oxidation by catalytically generating the long-chain acyl-CoA [20]. A deficiency in ACSL1-mediated long-chain acyl-CoA generation and fatty acid oxidation leads to ectopic lipid deposition, which is related to the pathogenesis of numerous diseases [42–44]. Defective lipid metabolism is closely related to tubulointerstitial fibrosis by

triggering EMT in renal tubular epithelial cells [45,46]. Ectopic lipid accumulation frequently occurs in tubulointerstitial fibrosis and the restoration of fatty acid metabolism protects against tubulointerstitial fibrosis [47]. In addition, ectopic lipid accumulation accelerates the proinflammatory response, which is also related to the development of tubulointerstitial fibrosis [48]. ACSL1 was down-regulated in obesity-associated nephropathy accompanied with increased lipid accumulation and triglyceride content [21]. The up-regulation of ACSL1 reduced lipid content in renal tubular epithelial cells stimulated by palmitic acid [21]. Moreover, the down-regulation of ACSL1 enhanced the progression of hepatic fibrosis by increasing lipid accumulation [49, 50]. However, the exact relevance of ACSL1 in tubulointerstitial fibrosis remains undetermined. This work demonstrated that ACSL1 expression

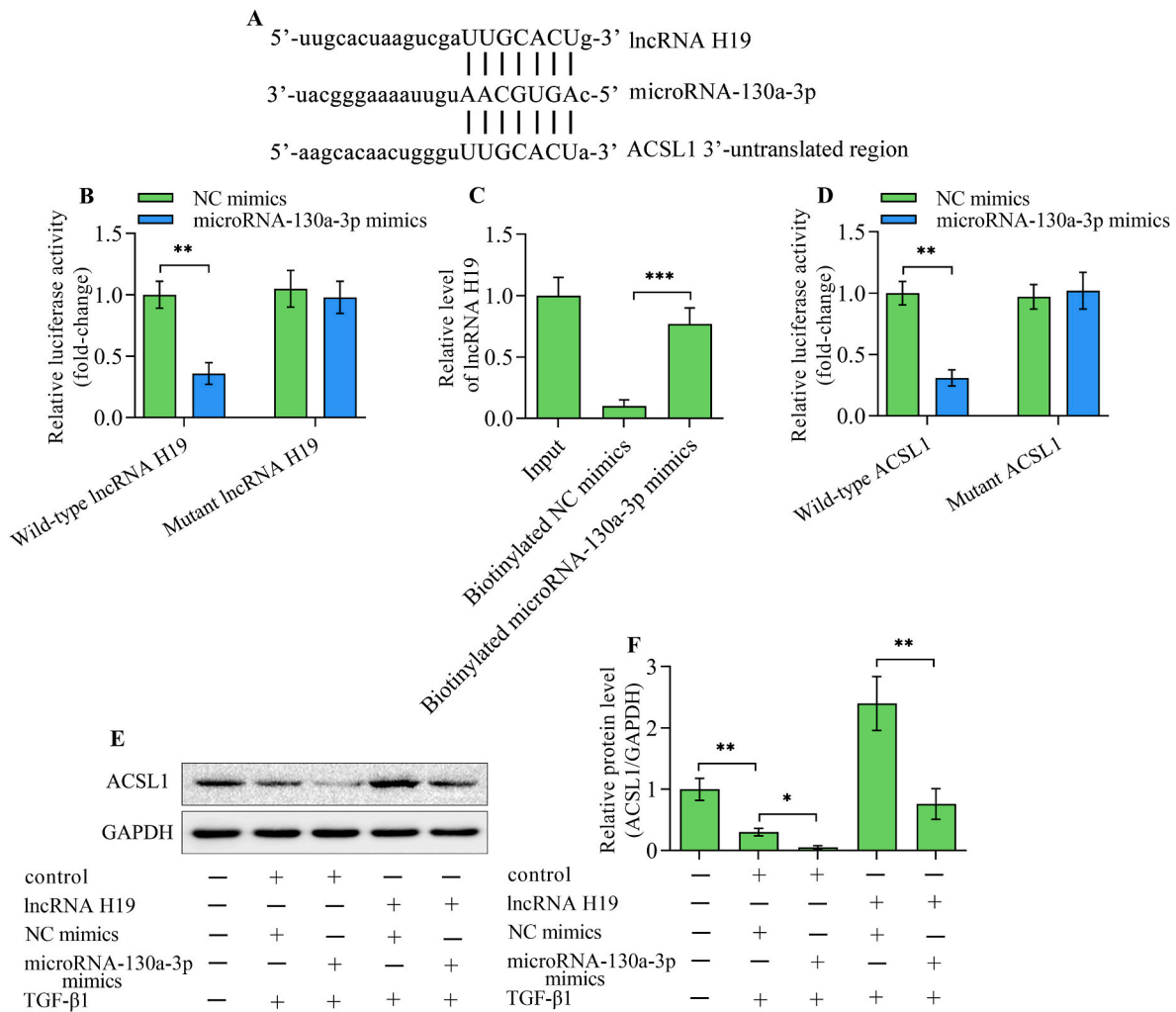


**Fig. 7.** lncRNA H19 mediates the expression of ACSL1 by microRNA-130a-3p. (A) Alignment between microRNA-130a-3p and lncRNA H19 or 3'-untranslated region of ACSL1. (B) A luciferase reporter assay was conducted in 293T cells co-transfected with negative control mimics or microRNA-130a-3p mimics and wild-type or mutant lncRNA H19 reporter plasmids (n = 3). (C) RNA pull-down assay was performed in HK-2 cells transfected with biotinylated negative control mimics or microRNA-130a-3p mimics. Levels of lncRNA H19 in RNA precipitants was assessed by quantitative real-time polymerase chain reaction (n = 3). (D) A luciferase reporter assay was carried out in 293T cells co-transfected with negative control mimics or microRNA-130a-3p mimics and wild-type or mutant ACSL1 3'-untranslated region reporter plasmids (n = 3). (E, F) HK-2 cells were co-transfected with adenoviruses expressing lncRNA H19 or control adenoviruses and negative control mimics or microRNA-130a-3p mimics before being stimulated with TGF-β1, and ACSL1 levels were detected using Western blotting (n = 3). Data were presented as mean ± standard deviation, \*p < 0.05, \*\*p < 0.01 and \*\*\*p < 0.001. ACSL1, long-chain acyl-CoA synthetase 1; NC mimics, negative control mimics; GAPDH, glyceraldehyde-3-phosphate dehydrogenase; TGF-β1, transforming growth factor-β1.

decreased in UUO kidneys and TGF-β1-stimulated HK-2 cells. The up-regulation of ACSL1 by lncRNA H19 contributed to reduction in tubulointerstitial fibrosis, lipid accumulation and inflammatory response in UUO kidneys. However, up-regulation of ACSL1 by lncRNA H19 under sham conditions did not impact the normal physical function of the kidney. Therefore, the function of lncRNA H19/ACSL1 is context-dependent. The abnormal expression of lncRNA H19/ACSL1 is not an initiator of the disease, but a regulator of the process. It functions only when the pathological process of renal tubulointerstitial fibrosis initiates. Furthermore, the silencing of ACSL1 enhanced TGF-β1-induced EMT and augmented lipid accumulation and inflammatory response. Collectively, these observations suggest that ACSL1-mediated lipid metabolism has a crucial role in tubulointerstitial fibrosis.

The work showed that lncRNA H19 overexpression increased the expression of ACSL1 in UUO kidneys and TGF-β1-stimulated HK-2 cells. The depletion of ACSL1 diminished the suppressive effect of lncRNA H19 on TGF-β1-induced EMT, lipid accumulation and inflammatory response. These findings confirm that lncRNA H19 mediates tubulointerstitial fibrosis via ACSL1. However, the precise regulatory

mechanism of lncRNA H19 on ACSL1 expression is unknown. The notable mechanism of lncRNA H19 in mediating gene expression is sponging microRNA [51,52]. Through bioinformatic analysis predictions, this work found that microRNA-130a-3p has the same binding sites for lncRNA H19 and 3'-untranslated region of ACSL1. The interaction between lncRNA H19 and microRNA-130a-3p was confirmed by using luciferase reporter assay and RNA pull-down assay. The luciferase reporter assay also provided evidence that microRNA-130a-3p has a direct interaction with 3'-untranslated region of ACSL1. Moreover, the overexpression of microRNA-130a-3p decreased the levels of ACSL1 and reversed the promoting effect of lncRNA H19 on ACSL1 expression, confirming that lncRNA H19 mediates the expression of ACSL1 via microRNA-130a-3p. Indeed, a suppressive function of microRNA-130a-3p on renal fibrosis has been documented. Levels of microRNA-130a-3p were up-regulated in renal tubular epithelial cells after TGF-β1 stimulation, and the inhibition of microRNA-130a-3p protected against TGF-β1-caused EMT [53]. Here, our work showed that microRNA-130a-3p promoted EMT, lipid accumulation and inflammatory response triggered by TGF-β1. Notably, the repressive

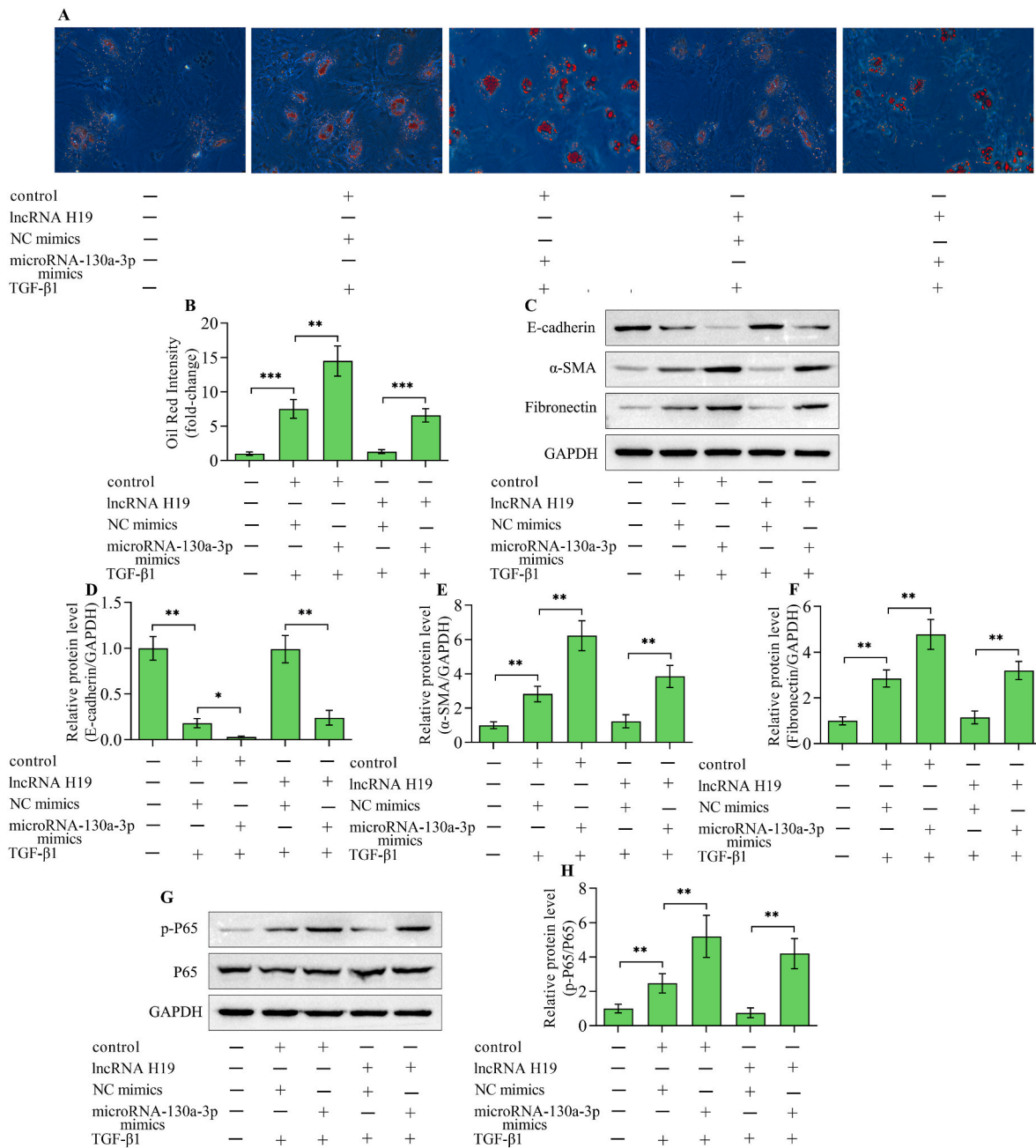


**Fig. 8.** microRNA-130a-3p reversed lncRNA H19-mediated effects. HK-2 cells were co-transfected with adenoviruses expressing lncRNA H19 or control adenoviruses and negative control mimics or microRNA-130a-3p mimics and then subjected to TGF-β1 stimulation. (A, B) Oil Red O staining of lipid deposition in HK-2 cells with different treatments (n = 3). (C) Western blotting detection and quantification of (D) E-cadherin, (E) α-smooth muscle actin and (F) fibronectin (n = 3). (G, H) Western blotting detection and quantification of nuclear factor-κB P65 (n = 3). Data were presented as mean ± standard deviation, \*p < 0.05 and \*\*p < 0.01. NC mimics, negative control mimics; TGF-β1, transforming growth factor-β1; α-SMA, α-smooth muscle actin; GAPDH, glyceraldehyde-3-phosphate dehydrogenase; P65, nuclear factor-κB P65.

impacts of lncRNA H19 on TGF-β1-triggered EMT, lipid accumulation and inflammatory response were also reversed by microRNA-130a-3p overexpression. Altogether, the findings of this work illustrate that lncRNA H19 increases the expression of ACSL1 by sponging microRNA-130a-3p, which may underlie lncRNA H19-mediated effects on tubulointerstitial fibrosis.

To conclude, this work showed that the up-regulation of lncRNA H19 protected against renal tubulointerstitial fibrosis. The renal-protective and anti-fibrosis function of lncRNA H19 is related to its regulatory effect on lipid deposition, which is achieved by increasing ACSL1 expression via sponging microRNA-130a-3p. The lncRNA H19/microRNA-130a-3p/ACSL1 axis-mediated reduction in lipid deposition

decreases the EMT of renal tubular epithelial cells and inflammatory response, which prevents the development of renal tubulointerstitial fibrosis. The work delineates a novel mechanism for lncRNA H19 in kidney tubulointerstitial fibrosis and proposes lncRNA H19 as a possible target for treating tubulointerstitial fibrosis.

**CRediT authorship contribution statement**

**Yali Jiang:** Writing – original draft, Investigation, Conceptualization. **Feng Ma:** Writing – original draft, Investigation, Conceptualization. **Jing Wang:** Writing – original draft, Investigation, Conceptualization. **Xiaojing Chen:** Writing – original draft,

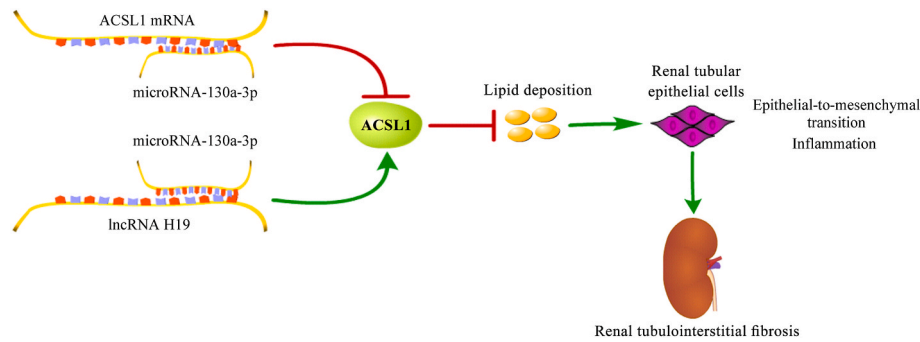


**Fig. 9.** A graphical model of lncRNA H19/microRNA-130a-3p/ACSL1 in renal tubulointerstitial fibrosis.

Investigation, Conceptualization. **Lu Xue:** Writing – original draft, Investigation, Conceptualization. **Xinping Chen:** Writing – original draft, Investigation, Conceptualization. **Jinping Hu:** Writing – review & editing, Conceptualization.

#### Declaration of competing interest

The authors declare that they have no known competing financial interests or personal relationships that could have appeared to influence the work reported in this paper.

#### Acknowledgement

This work was supported by Natural Science Basic Research Program of Shaanxi Province (Program No. 2023-JC-QN-0843).

#### References

- [1] B.D. Humphreys, Mechanisms of renal fibrosis, *Annu. Rev. Physiol.* 80 (2018) 309–326.
- [2] G.B.D.C.K.D. Collaboration, Global, regional, and national burden of chronic kidney disease, 1990–2017: a systematic analysis for the Global Burden of Disease Study 2017, *Lancet* 395 (2020) 709–733.
- [3] A.S. Cruz-Solbes, K. Youker, Epithelial to mesenchymal transition (EMT) and endothelial to mesenchymal transition (EndMT): role and implications in kidney fibrosis, *Results Probl. Cell Differ.* 60 (2017) 345–372.
- [4] P. Ruffo, F. De Amicis, E. Giardina, et al., Long-noncoding RNAs as epigenetic regulators in neurodegenerative diseases, *Neural Regen Res* 18 (2023) 1243–1248.
- [5] K. Li, Z. Wang, lncRNA NEAT1: key player in neurodegenerative diseases, *Ageing Res. Rev.* 86 (2023) 101878.
- [6] A. Mangiavacchi, G. Morelli, V. Orlando, Behind the scenes: how RNA orchestrates the epigenetic regulation of gene expression, *Front. Cell Dev. Biol.* 11 (2023) 1123975.
- [7] I.M. Dykes, C. Emanuelli, Transcriptional and post-transcriptional gene regulation by long non-coding RNA, *Dev. Reprod. Biol.* 15 (2017) 177–186.
- [8] L.P. Lim, N.C. Lau, P. Garrett-Engel, et al., Microarray analysis shows that some microRNAs downregulate large numbers of target mRNAs, *Nature* 433 (2005), 769–673.
- [9] W. Xia, Y. He, Y. Gan, et al., Long non-coding RNA: an emerging contributor and potential therapeutic target in renal fibrosis, *Front. Genet.* 12 (2021) 682904.
- [10] H. Chen, Y. Fan, H. Jing, et al., Emerging role of lncRNAs in renal fibrosis, *Arch. Biochem. Biophys.* 692 (2020) 108530.
- [11] D. Busscher, R.A. Boon, R.P. Juni, The multifaceted actions of the lncRNA H19 in cardiovascular biology and diseases, *Clin. Sci. (Lond.)* 136 (2022) 1157–1178.
- [12] Y. Bi, Y. Wang, X. Sun, Recent advances of lncRNA H19 in diabetes lncRNA H19 in diabetes, *Horm. Metab. Res.* 54 (2022) 212–219.
- [13] L. Zhong, P. Liu, J. Fan, et al., Long non-coding RNA H19: physiological functions and involvements in central nervous system disorders, *Neurochem. Int.* 148 (2021) 105072.
- [14] X. Dong, R. Cao, Q. Li, et al., The long noncoding RNA-H19 mediates the progression of fibrosis from acute kidney injury to chronic kidney disease by regulating the miR-196a/Wnt/beta-Catenin signaling, *Nephron* 146 (2022) 209–219.
- [15] Y. Yuan, X. Li, Y. Chu, et al., Long non-coding RNA H19 augments hypoxia/reoxygenation-induced renal tubular epithelial cell apoptosis and injury by the miR-130a/bcl2l1 pathway, *Front. Physiol.* 12 (2021) 632398.
- [16] L. Jiang, W. Wei, S. Kang, et al., Insights into lipid metabolism and immune-inflammatory responses in the pathogenesis of coronary artery ectasia, *Front. Physiol.* 14 (2023) 1096991.
- [17] S.S. Abdalla, A.A. Harb, I.M. Almasri, et al., The interaction of TRPV1 and lipids: insights into lipid metabolism, *Front. Physiol.* 13 (2022) 1066023.
- [18] M. Rossi Sebastiano, G. Konstantinidou, Targeting long chain acyl-CoA synthetases for cancer therapy, *Int. J. Mol. Sci.* 20 (2019) 3624.
- [19] E. Soupene, F.A. Kuypers, Mammalian long-chain acyl-CoA synthetases, *Exp. Biol. Med.* 233 (2008) 507–521.
- [20] S. Zeng, F. Wu, M. Chen, et al., Inhibition of fatty acid translocase (FAT/CD36) palmitoylation enhances hepatic fatty acid beta-oxidation by increasing its localization to mitochondria and interaction with long-chain acyl-CoA synthetase 1, *Antioxidants Redox Signal.* 36 (2022) 1081–1100.
- [21] Y. Chen, L. He, Y. Yang, et al., The inhibition of Nrf2 accelerates renal lipid deposition through suppressing the ACSL1 expression in obesity-related nephropathy, *Ren. Fail.* 41 (2019) 821–831.
- [22] L. Ren, H. Cui, Y. Wang, et al., The role of lipotoxicity in kidney disease: from molecular mechanisms to therapeutic prospects, *Biomed. Pharmacother.* 161 (2023) 114465.
- [23] H. Nishi, T. Higashihara, R. Inagi, Lipotoxicity in kidney, heart, and skeletal muscle dysfunction, *Nutrients* 11 (2019) 1664.
- [24] E. Escasany, B. Lanzon, A. Garcia-Carrasco, et al., Transforming growth factor beta3 deficiency promotes defective lipid metabolism and fibrosis in murine kidney, *Dis Model Mech* 14 (2021) dmm048249.
- [25] L. Liu, X. Ning, L. Wei, et al., Twist1 downregulation of PGC-1alpha decreases fatty acid oxidation in tubular epithelial cells, leading to kidney fibrosis, *Theranostics* 12 (2022) 3758–3775.
- [26] L. Chen, M.L. Sha, F.T. Chen, et al., Upregulation of KLF14 expression attenuates kidney fibrosis by inducing PPARalpha-mediated fatty acid oxidation, *Free Radic. Biol. Med.* 195 (2023) 132–144.
- [27] X. Jiang, Q. Ning, The mechanism of lncRNA H19 in fibrosis and its potential as novel therapeutic target, *Mech. Ageing Dev.* 188 (2020) 111243.
- [28] L. He, H. Wang, P. He, et al., Serum long noncoding RNA H19 and CKD progression in IgA nephropathy, *J. Nephrol.* 36 (2023) 397–406.
- [29] R.L. Chevalier, M.S. Forbes, B.A. Thornhill, Ureteral obstruction as a model of renal interstitial fibrosis and obstructive nephropathy, *Kidney Int.* 75 (2009) 1145–1152.
- [30] C.A. Laferriere, D.S. Pang, Review of intraperitoneal injection of sodium pentobarbital as a method of euthanasia in laboratory rodents, *J Am Assoc Lab Anim Sci* 59 (2020) 254–263.
- [31] S.E. McGeary, K.S. Lin, C.Y. Shi, et al., The biochemical basis of microRNA targeting efficacy, *Science* 366 (2019) eaav1741.
- [32] J.H. Li, S. Liu, H. Zhou, et al., starBase v2.0: decoding miRNA-ceRNA, miRNA-ncRNA and protein-RNA interaction networks from large-scale CLIP-Seq data, *Nucleic Acids Res.* 42 (2014) D92–D97.
- [33] J. Li, L.T. Cao, H.H. Liu, et al., Long non coding RNA H19: an emerging therapeutic target in fibrosis diseases, *Autoimmunity* 53 (2020) 1–7.
- [34] N. Thipboonchoo, S. Fongsupa, S. Sureram, et al., Altenusin, a fungal metabolite, alleviates TGF-beta1-induced EMT in renal proximal tubular cells and renal fibrosis in unilateral ureteral obstruction, *Heliyon* 10 (2024) e24983.
- [35] S. Lu, X. Chen, Y. Chen, et al., Downregulation of PDZK1 by TGF-beta1 promotes renal fibrosis via inducing epithelial-mesenchymal transition of renal tubular cells, *Biochem. Pharmacol.* 220 (2024) 116015.
- [36] L. Hou, Y. Du, Neurophilin 1 promotes unilateral ureteral obstruction-induced renal fibrosis via RACK1 in renal tubular epithelial cells, *Am. J. Physiol. Ren. Physiol.* 325 (2023) F870–F884.
- [37] S. Yang, G. Yang, X. Wang, et al., SIRT2 alleviated renal fibrosis by deacetylating SMAD2 and SMAD3 in renal tubular epithelial cells, *Cell Death Dis.* 14 (2023) 646.
- [38] S. Hadjpech, V. Thongboonkerd, Epithelial-mesenchymal plasticity in kidney fibrosis, *Genesis* (2023) e23529.
- [39] L. Xiong, Y. Sun, J. Huang, et al., Long non-coding RNA H19 prevents lens fibrosis through maintaining lens epithelial cell phenotypes, *Cells* 11 (2022) 2559.
- [40] T. Iempridee, Long non-coding RNA H19 enhances cell proliferation and anchorage-independent growth of cervical cancer cell lines, *Exp. Biol. Med.* 242 (2017) 184–193.
- [41] S. Shi, L. Song, H. Yu, et al., Knockdown of lncRNA-H19 ameliorates kidney fibrosis in diabetic mice by suppressing miR-29a-mediated EndMT, *Front. Pharmacol.* 11 (2020) 586895.
- [42] H. Dong, W. Zhong, W. Zhang, et al., Loss of long-chain acyl-CoA synthetase 1 promotes hepatocyte death in alcohol-induced steatohepatitis, *Metabolism* 138 (2023) 155334.
- [43] J.E. Kanter, C. Tang, J.F. Oram, et al., Acyl-CoA synthetase 1 is required for oleate and linoleate mediated inhibition of cholesterol efflux through ATP-binding

- cassette transporter A1 in macrophages, *Biochim. Biophys. Acta* 1821 (2012) 358–364.
- [44] J. Nan, J.S. Lee, S.A. Lee, et al., An essential role of the N-terminal region of ACSL1 in linking free fatty acids to mitochondrial beta-oxidation in C2C12 myotubes, *Mol. Cell.* 44 (2021) 637–646.
- [45] Q. Ke, Q. Yuan, N. Qin, et al., UCP2-induced hypoxia promotes lipid accumulation and tubulointerstitial fibrosis during ischemic kidney injury, *Cell Death Dis.* 11 (2020) 26.
- [46] Y. Ruan, P.P. Yuan, Y.X. Wei, et al., Phenolic Compounds from Mori Cortex Ameliorate Sodium Oleate-Induced Epithelial-Mesenchymal Transition and Fibrosis in NRK-52e Cells through CD36, *Molecules* 26 (2021) 6133.
- [47] H.M. Kang, S.H. Ahn, P. Choi, et al., Defective fatty acid oxidation in renal tubular epithelial cells has a key role in kidney fibrosis development, *Nat. Med.* 21 (2015) 37–46.
- [48] Z. Cao, H. Zhao, J. Fan, et al., Simultaneous blockade of VEGF-B and IL-17A ameliorated diabetic kidney disease by reducing ectopic lipid deposition and alleviating inflammation response, *Cell Death Dis.* 9 (2023) 8.
- [49] B. Li, J. Liu, X. Xin, et al., MiR-34c promotes hepatic stellate cell activation and Liver Fibrogenesis by suppressing ACSL1 expression, *Int. J. Med. Sci.* 18 (2021) 615–625.
- [50] W.Q. Li, C. Chen, M.D. Xu, et al., The rno-miR-34 family is upregulated and targets ACSL1 in dimethylnitrosamine-induced hepatic fibrosis in rats, *FEBS J.* 278 (2011) 1522–1532.
- [51] Y. Wang, J. Zeng, W. Chen, et al., Long noncoding RNA H19: a novel oncogene in liver cancer, *Noncoding RNA* 9 (2023) 19.
- [52] M. Shirvaliloo, LncRNA H19 promotes tumor angiogenesis in smokers by targeting anti-angiogenic miRNAs, *Epigenomics* 15 (2023) 61–73.
- [53] K. Ai, X. Zhu, Y. Kang, et al., miR-130a-3p inhibition protects against renal fibrosis in vitro via the TGF-beta1/Smad pathway by targeting SnoN, *Exp. Mol. Pathol.* 112 (2020) 104358.